Available online at www.sciencedirect.com

SCIENCE DIRECT®

Catalysis Today 101 (2005) 147–154

CATALYSIS TODAY

www.elsevier.com/locate/cattod

Dealumination of ferrierite type zeolite: Physicochemical and catalytic properties

R. Rachwalik [a], Z. Olejniczak [b], B. Sulikowski [a,*]

[a] *Institute of Catalysis and Surface Chemistry, Polish Academy of Sciences, Niezapominajek 8, 30-239 Kraków, Poland*
[b] *Institute of Nuclear Physics, Polish Academy of Sciences, Radzikowskiego 152, 31-342 Kraków, Poland*

Abstract

Dealumination of ferrierite type zeolite was studied using aqueous solutions of hydrochloric acid of different concentrations. The course of the reaction was monitored by XRD, sorption, NMR, XPS and TPD of ammonia. The catalytic properties were studied using *m*-xylene transformations as a test reaction. A mild treatment with the diluted acid exerts a significant effect on the reaction path. The selectivity towards *p*-xylene formation on the dealuminated samples was strongly preferred and much greater than thermodynamic equilibrium data. Simultaneously, disproportionation of *m*-xylene yielding toluene and trimethylbenzenes was suppressed.

Keywords: Ferrierite; Dealumination; Hydrochloric acid; NMR; Xylenes; Isomerization; Disproportionation

1. Introduction

The framework of zeolites is amenable to modification carried out either during the synthesis or post-synthesis treatments, thus yielding a practically infinite number of their variants. In particular, (hydro)thermal or chemical treatment of a zeolite leads inevitably to a change of its Si/Al framework ratio. This is a fundamental property of aluminosilicates, which governs to a large extent their stability, sorption and catalytic properties. A number of studies were therefore devoted to the processes aimed at the Si/Al manipulation in zeolites [1]. Several processes focused on this objective were developed, starting from either the siliceous (realumination process) or the aluminous (dealumination process) end-members of zeolite substitutional series, and yielding the modified solids with desired silicon and aluminium content [2].

The earliest contribution to this field was made by Barrer and Makki [3], who treated natural clinoptilolite by hydrochloric acid and obtained a series of highly crystalline solids with progressively changed adsorption properties. Dealumination of different zeolites by acids was studied, including ZSM-5 [4] and faujasite [5–7], to name a few. It is now clear that these processes occur to a different degree, taking into account the conditions applied, the Si/Al ratio in a starting material, and first of all the zeolite structure. The conditions giving excellent results in one zeolite can yield quite unsatisfactory results when applied to another structure. Finally, some of the dealumination processes were implemented industrially, and catalysts with high activity and selectivity are now manufactured [8].

Various transformations of alkylaromatic hydrocarbons are known to proceed readily on Brønsted acid sites. Such sites can be distributed either in amorphous or crystalline aluminosilicates (zeolites), or in a number of other solids, including mesoporous molecular sieves. The transformations of alkylaromatics [9] can be therefore used conveniently to monitor the behaviour of acid sites in different classes of molecular sieves, brought about by their modification. The reactions of alkylaromatics comprise isomerization, transalkylation, disproportionation and dealkylation. Of these, the isomerization of dialkylbenzenes in general, and dimethylbenzenes (xylenes) in particular, is an important reaction carried out at the industrial scale worldwide. Moreover, the isomerization of xylenes is used as an excellent test reaction, applied successfully to monitor acidity and shape-selectivity of the modified solids [10–13].

---

* Corresponding author. Tel.: +48 12 6395127; fax: +48 12 4251923.
E-mail address: ncsuliko@cyf-kr.edu.pl (B. Sulikowski).

0920-5861/$ – see front matter © 2005 Elsevier B.V. All rights reserved.
doi:10.1016/j.cattod.2005.01.012

Ferrierite (FER) is a medium-pore zeolite, with smaller pore openings than ZSM-5. It is quite distinct from most zeolites as the four-membered rings are not present in its structure (in other words, the five-membered rings are the smallest ones building its three-dimensional framework). Ferrierite is noticeable as having a stable structure and hence constitutes a promising object for fundamental and applied studies. The catalytic reactions proceeding readily on this zeolite are: isomerization of 1-butene, *n*-octane cracking, NO removal and oxidative dehydrogenation of propane [14–17].

The objective of this work was to study dealumination of ferrierite by hydrochloric acid solutions using different techniques and monitor the catalytic properties of the resultant solids in *m*-xylene transformations.

2. Experimental

2.1. Samples preparation

The ammonium form of ferrierite with the Si to Al molar ratio of 10 (from Zeolyst, USA) was treated with the 0.25–11.4 M HCl hydrochloric acid solutions at ambient temperature with stirring for 4 h. During this treatment, the ratio of the acid solution to zeolite was kept at 30 cm^3 for 1 g of the sample. After dealumination, the samples were thoroughly washed with distilled water and dried at 353 K overnight. Finally, all the samples prior to further characterization and catalytic tests were calcined in air at 773 K for 5 h.

2.2. X-ray diffraction

Powder X-ray diffraction patterns (XRD) of the hydrated samples were obtained by using a Siemens D5005 automatic diffractometer with Cu Kα radiation (up to 50° 2Θ). Silicon powder was used as the internal standard, in quantity of 15 wt.%, for calibration of the diffraction angle, calculation of the unit cell parameters and estimation of the crystallinity of dealuminated zeolites. The main signals corresponding to various $h\,k\,l$ values were chosen at $d = 0.954$, 0.714, 0.706, 0.659, 0.585, 0.570, 0.401, 0.396, 0.382, 0.380, 0.366, 0.355, 0.347, 0.336, 0.331, 0.313 and 0.305 nm ($h\,k\,l = 2\,0\,0$, 0 2 0, 1 0 1, 0 1 1, 3 1 0, 2 2 0, 0 3 1, 4 2 0, 4 1 1, 3 3 0, 5 1 0, 0 4 0, 2 0 2, 5 0 1, 2 4 0, 2 2 2 and 5 2 1, respectively). The intensity of each reflection was related to zeolite and silicon powder used as the internal standard ($2\Theta = 28.30°$). Standard deviations, σ, for unit cell constants *a*, *b*, *c* were 0.0003, 0.0007 and 0.0009 Å, respectively.

2.3. BET

Sorption of nitrogen was studied using Quantachrome Autosorb Automated Gas Sorption System. Prior to measurement the samples were outgassed at 473 K for 24 h. Values of the external surface area (S_E), micro-pore area (S_μ), total pore volume (V_T) and micro-pore volume (V_μ) were estimated by applying the *t*-method micropore analysis according to de Boer.

2.4. XPS

XPS was performed with a SSI X-probe (SSX-100/206) spectrometer from Surface Science Instruments working with a monochromatic Al Kα radiation (10 kV, 22 mA). Charge compensation was achieved by using an electron flood gun adjusted at 8 eV and placing a nickel grid 3.0 mm above the sample. Energy of pass for the analyser was 50 eV and the spot size was 1000 mm in diameter, corresponding to a full width at half maximum (FWHM) of 1.1 eV for the Au $4f_{7/2}$ band of a gold standard. For these experiments, O 1s, C 1s, Si 2p and Al 2p bands were recorded.

2.5. TPD of ammonia

The TPD of ammonia of ferrierite samples (weight 0.250 mg) was carried out in a stream of helium (30 cm^3/min) at a heating rate of 3 K/min. Prior to TPD, the samples were activated at 773 K for 3 h and cooled to 298 K in a helium flow. Ammonia was then passed over the samples for 15 min, followed by the temperature increase to 453 K, and the samples were purged with helium for 3 h at 453 K in order to eliminate physisorbed species. Finally, the temperature was increased at 3 K/min from 453 to 923 K and the TPD data were acquired.

2.6. NMR spectroscopy

Solid-state magic-angle-spinning nuclear magnetic resonance (MAS NMR) spectra were measured on a home-made pulse NMR spectrometer at the magnetic field of 7.05 T. A Bruker HP-WB high-speed MAS probe equipped with the 4 mm zirconia rotor and KEL-F cap was used to record the MAS spectra at the spinning speed ranging from 4 to 7 kHz. All the NMR spectra shown here were normalised, taking into account the acquisition numbers and the sample weight.

2.7. FT-IR spectroscopy

The IR spectra of the zeolite framework vibration region were obtained with a Nicolet 800 FT spectrometer, using the samples pelletized with KBr.

2.8. Catalytic tests

The isomerization reactions were carried out in a tabular down-flow stainless steel reactor with 50 mg of catalyst (200–315 μm fraction) and 2 cm^3 of SiC chips (>400 μm fraction). A catalyst was activated in helium flow (30 cm^3/min) at 753 K for 1 h. After pre-treatment the temperature was decreased to 623 K and 10 injections of a 10 μl substrate were applied in the 1 min sequence to stabilise the performance of catalysts. Then the temperature was decreased further to 523 K and the catalytic tests were performed at the 523–723 K temperature range under flowing helium (30 cm^3/min).

2.9. Isomerization of m-xylene

The *m*-xylene conversion and the selectivity of *p*-xylene formation were calculated as shown below:

$$X_{m\mathrm{X}} = \left[\frac{98.62 - c_{m\mathrm{X}}}{98.62}\right]100\%, \qquad \frac{p\text{-xylene}}{o\text{-xylene}} = \frac{c_{p\mathrm{X}} - 0.93}{c_{o\mathrm{X}} - 0.45},$$

$$S_{p\mathrm{X}} = \left[\frac{c_{p\mathrm{X}} - 0.93}{98.62 - c_{m\mathrm{X}}}\right]100\%$$

where $X_{m\mathrm{X}}$ denotes the conversion of *m*-xylene (mol%) and $S_{p\mathrm{X}}$ the selectivity of *p*-xylene formation (mol%); *p*-xylene/*o*-xylene the *para*- to *ortho*-xylene molar ratio; $c_{m\mathrm{X}}$, $c_{p\mathrm{X}}$, and $c_{o\mathrm{X}}$ are the concentrations (mol%) of *m*-, *p*-, and *o*-xylene in the products, respectively. The concentrations of *m*-xylene, *p*-xylene and *o*-xylene in the feed were 98.62, 0.93 and 0.45 mol%, respectively.

3. Results and discussion

When considering a treatment of any aluminosilicate the most important factor constitutes resistance of its framework against the acid. It is known that some zeolites (e.g., faujasite) are not very stable even against mild acids, like H_4EDTA [2]. There are various routes to avoid excessive collapse of the zeolite framework. The parent sample has to be already siliceous, or the treatment must be performed in steps, thus increasing the severity of the treatment with dealumination progress (cf. ultrastabilization of zeolite Y [1]). To address this question, the parent ferrierite was subjected to HCl solution treatment over a large range of acid concentration (0.25–11.4 M), while keeping the other parameters fixed (4 h reaction time, room temperature). As shown in Table 1, the loss of aluminium from framework increases with the concentration of hydrochloric acid. Contrary to expectation, the dealumination begins already at relatively low concentration of acid. All the modified samples exhibit high crystallinity with increased severity of the acid treatment. This is visualized in XRD patterns of the samples in Fig. 1, while the quantitative data are listed in Table 1. The loss of crystallinity for most of the samples is well below 10%, and the highest loss equal to 17% was obtained for one sample after the treatment with concentrated 10 M HCl solution (Table 1).

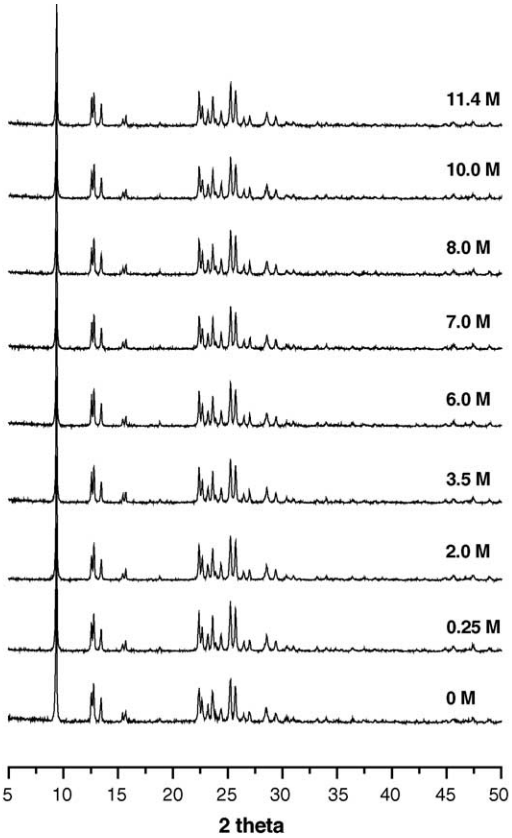

Fig. 1. X-ray diffraction patterns of the parent and dealuminated forms of ferrierite.

In general, dealumination affects the unit cell parameters of zeolites. As the Si–O bond is longer than Al–O, a

Table 1
Characteristic of the parent hydrogen ferrierite H–FER and its dealuminated forms

Sample	XRD crystallinity (%)	Unit cell parameter (Å)			Unit cell volume ($Å^3$)	Si/Al_{XPS}	Si/Al_{NMR}	Tetrahedral framework aluminium[a] removed (wt.%)
		a	*b*	*c*				
H–FER	100	18.914	14.120	7.451	1989.9	10.1	10.0	0
NH_4–FER (0.25 HCl/4 h)	97	18.886	14.100	7.448	1983.4	10.9	12.5	18
NH_4–FER (2.0 HCl/4 h)	96	18.880	14.100	7.446	1982.2	12.1	12.5	20
NH_4–FER (3.5 HCl/4 h)	95	18.880	14.099	7.448	1982.6	11.9	13.1	24
NH_4–FER (6.0 HCl/4 h)	93	18.876	14.096	7.447	1981.5	11.7	13.5	26
NH_4–FER (7.0 HCl/4 h)	91	18.881	14.095	7.445	1981.3	11.5	14.3	30
NH_4–FER (8.0 HCl/4 h)	94	18.875	14.096	7.446	1981.1	11.4	–	100
NH_4–FER (10.0 HCl/4 h)	83	18.740	14.094	7.446	1966.5	11.6	18.9	47
NH_4–FER (11.4 HCl/4 h)	91	18.878	14.094	7.446	1981.1	11.1	13.2	24

[a] Calculated from quantitative deconvolution of the ^{27}Al MAS NMR spectra.

contraction of the framework is expected and observed. The acid treatment of ferrierite exerts only a very small effect on the unit cell parameters of the modified samples (Table 1). As seen, the contraction of the FER framework proceeds in an anisotropic way, and the more pronounced changes were observed along the *a*-axis. This is in accord with observations made earlier for zeolite MFI with the pentasil type structure. It was demonstrated for the doubly substituted [B, Al]-ZSM-5 solids [18] that the framework expansion/contraction were having anisotropic character upon various boron, aluminium and silicon substitutions in the ZSM-5 crystals. Similar observations were noted for other zeolites, e.g. mordenite [19]. The unit cell volumes of the dealuminated samples were calculated and are shown in Table 2. There is a constant, albeit small, contraction of the u.c. volume upon increasing the severity of the treatment. A sample leached with 10 M HCl solution is an exception, and here a higher contraction of the u.c. is observed accompanied by larger crystallinity loss. Similar observations were made for dealuminated samples, where a very small effect unit cell contraction was found upon leaching ZSM-5 with HCl [20].

Adsorption and porosity characteristics of the parent and dealuminated samples derived from nitrogen adsorption–desorption isotherms at 77 K are given in Table 2. These data reveal that the dealumination process, to which ferrierite was subjected, significantly affect neither total – external and micropore surface areas – nor the total pore volume. The BET area is around 300 m^2/g for the parent and dealuminated forms, and all the samples are characterised by good sorption properties (cf. micro-pore volume V_μ in Table 2).

The ^{29}Si MAS NMR spectra are given in Fig. 2. The trace of H–FER consists of a broad, asymmetric signal due to Si(0Al), Si(1Al) and Si(2Al) unresolved components. The character of the signal changes slightly upon treatment with increased concentration of HCl. We note the resolution is better for samples treated with the more concentrated acid solutions (8–11.4 M).

The evolution of the ^{27}Al MAS NMR signals is visualized in absolute scale in Fig. 3. A continuous decrease of the intensity of tetrahedral framework aluminium is observed. The process is monotonous until 7 M HCl. A very interesting sample was obtained after treating ferrierite 8 M aqueous solution of hydrochloric acid. The ^{27}Al MAS NMR spectrum of this sample, contrary to expectations, does not exhibit any signal typical for aluminium species in any possible coordination (tetrahedral, pentahedral or octahedral). It is therefore evident that the symmetry of such Al must be highly distorted; hence the NMR signal of the quadrupolar nuclei is too broad to be observed experimentally. Further experiment using even more concentrated acid leads to 47% aluminium removal (Table 1), while for 11.4 M HCl dealumination is not so advanced (24%, similar to the effect of 3.5 M HCl). At present there is no explanation of such an anomalous behaviour.

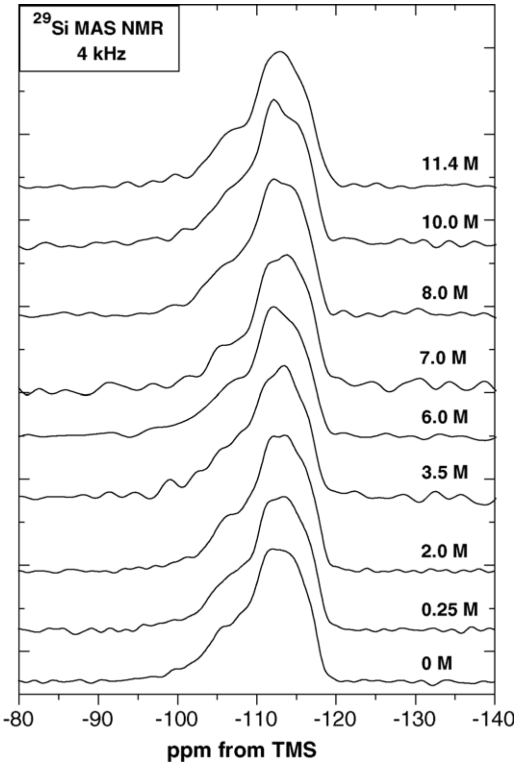

Fig. 2. ^{29}Si MAS NMR spectra of H–ferrierite and its dealuminated forms.

Table 2
Characteristics of porosity of the zeolite H–FER and dealuminated catalysts

Sample	BET (m^2/g)	S_E (m^2/g)[a]	S_μ (m^2/g)[b]	V_T (cm^3/g)[c]	V_μ (cm^3/g)[d]
H–FER	287.4	40.0	247.4	0.2428	0.1287
NH_4–FER (0.25 HCl/4 h)	311.4				
NH_4–FER (2.0 HCl/4 h)	281.0	39.3	241.7	0.2620	0.1330
NH_4–FER (3.5 HCl/4 h)	300.1				
NH_4–FER (6.0 HCl/4 h)	299.9	38.6	261.5	0.2447	0.1349
NH_4–FER (7.0 HCl/4 h)	307.2				
NH_4–FER (8.0 HCl/4 h)	300.5	37.7	262.8	0.2235	0.1362
NH_4–FER (10.0 HCl/4 h)	299.3				
NH_4–FER (11.4 HCl/4 h)	297.0	38.0	243.5	0.2741	0.1354

[a] S_E – external surface area.
[b] S_μ – micro-pore area.
[c] V_T – total pore volume.
[d] V_μ – micro-pore volume.

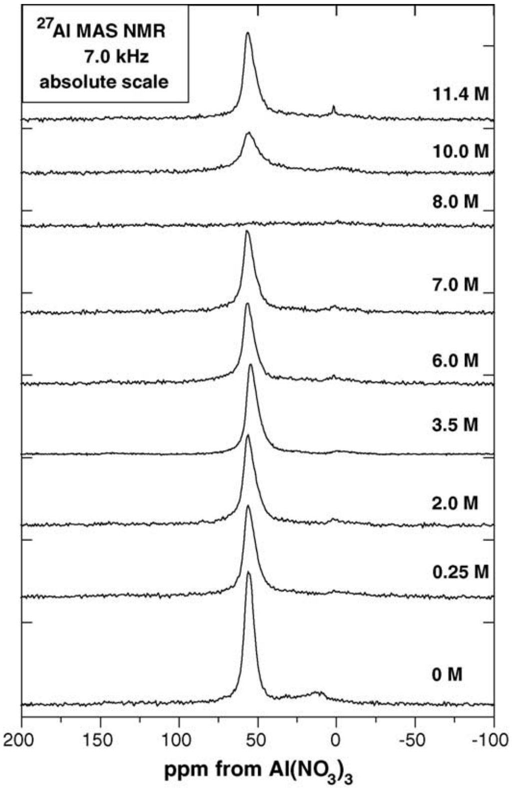

Fig. 3. ^{27}Al MAS NMR spectra of ferrierite samples.

Thus summarizing, 47% of dealumination was achieved in ferrierite, and the Si/Al$_F$ ratio has changed from initial 10 to 18.9 after the treatment. This is a substantial increase, in comparison with other reagents used for dealumination, like ammonium hexafluorosilicate [21].

Framework vibration modes were studied by IR spectroscopy and are shown in Fig. 4. In general, all the samples obtained exhibit well-resolved bands confirming their high crystallinity. The main signals were found at 1099, 585 and 470 cm^{-1}. The HCl treatment does affect neither the shape nor the position of the signals. This is in line with characteristics of the samples obtained by XRD and sorption of nitrogen.

The outer surface of zeolite crystals was monitored by XPS and compared with NMR data (Table 1). It is clear that the XPS Si/Al ratios are systematically lower than the bulk ratio estimated by NMR. Such a finding points out to the slight enrichment of the crystals surface in aluminium, expelled from the tetrahedral positions and transported towards the surface during the acid treatment. Additionally, by using higher concentrations of hydrochloric acid the silicon atoms are also removed. This slight decrease of Si concentration in the samples is negligible for NMR, but important for XPS technique. A reproducibility of the unexpected behaviour of the ferrierite treated with 8 M HCl was re-checked, by repeating the dealumination experiments using the following acid concentrations: 6, 7 and 8 M HCl. The results obtained were the same—the sample treated with 8 M HCl revealed the same unusual characteristics as before.

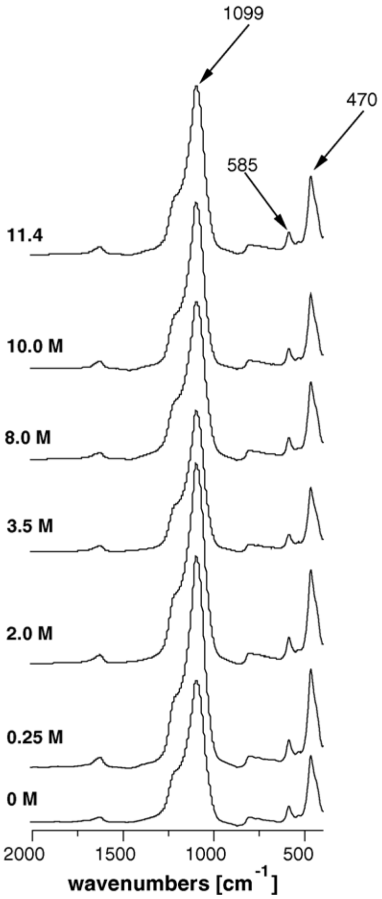

Fig. 4. FT-IR spectra of ferrierite samples.

The acidity of the parent sample H–FER and dealuminated ferrierites was estimated by temperature-programmed desorption (TPD) of ammonia. The NH$_3$-TPD patterns are shown in Fig. 5. In all the profiles a first signal is found around 500 K, followed by two or three peaks in the high temperature region. In the NH$_3$-TPD profiles of zeolite hydrogen forms the two regions can be discerned, a low temperature (LT) and a high temperature one HT (>673 K). There is general agreement that the HT signals are due to the zeolite Brønsted and Lewis acid centres, while the assign-

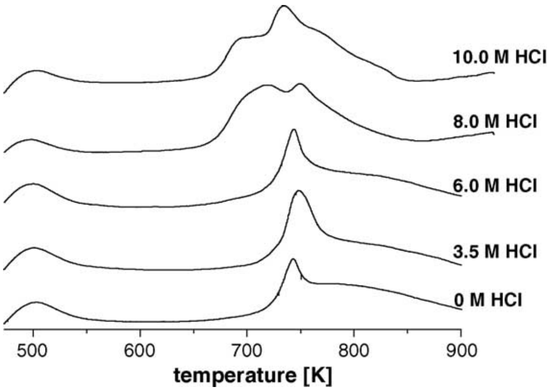

Fig. 5. TPD-NH$_3$ profiles of ferrierite samples.

ment of signals in the LT is a matter of discussion. Here different factors might be taken into account, we note, however, that the conditions of the experiments are important, especially the heating rate. Many published data were collected at high heating rate of 10 K/min [14,22]. Our experiments were carried out using 3 K/min only. Under these conditions a good resolution was obtained. This is somewhat similar to the situation found in derivatography, where artefacts were frequently encountered, if experiments were performed using the high heating rate. Thus for H–FER three signals were found (Fig. 4a), at 520, 740 and 820 K. The first signal is assigned to weak adsorption of ammonia, probably physisorption. The two other signals are due to the Brønsted acid centres. If the heating rate is faster, the coalescence of the two HT signals is observed [14]. Ferrierite is a very stable structure. At $t = 773$ K no dehydroxylation was found, according to our ^{27}Al NMR data and literature reference [23]. This process was observed in our samples at much higher temperature of 923 K.

The first signal around 500 K was found in the all dealuminated samples. It is well known that during dealumination weak and medium acid centres are removed from zeolite first [2,22,24]. The origin of this signal is therefore not due to the weak zeolite acidity, but rather due to ammonia physisorption, in accord with TPD experiments performed on ZSM-5 and mordenite [25]. In the HT region one narrow signal is accompanied by a broad one for the samples treated with 3.5 and 6 M HCl. The TPD profile becomes more complicated after treatment with more concentrated acid (>6 M). Here additional signals were observed at about 720 K. Moreover, the shoulders at 773 and 820 K are much more pronounced (Fig. 4d and e). The first signal at 720 K can be assigned to Brønsted acid centres located on the framework tetrahedral Al, while the second at 750 K to the extra framework acid sites [14,26]. These experiments reveal therefore the presence of Brønsted acid sites located on a highly distorted Al, which cannot be detected by standard ^{27}Al NMR acquisition (the sample treated with 8 M HCl gives no aluminium signal, Fig. 3g).

Catalytic properties of representative samples are summarized in Figs. 6 and 7. The main products of *m*-xylene transformation are the *p*- and *o*-xylene. A small amount of toluene and trimethylbenzenes, resulting from xylene disproportionation, is also detected. The highest conversion (up to 25%) was found for the hydrogen form of parent ferrierite. Treatment with 0.25 HCl decreases the conversion to 21% (at 773 K), while more intensive leaching (8 M HCl) leads to almost the same catalytic activity (Fig. 6).

p-Xylene/*o*-xylene ratio is plotted versus HCl concentration and here an abrupt change of the ratio is observed already for the 0.25 M HCl-treated sample (Fig. 7a). Then the ratio levels out around this value (2.6) for 10% conversion and 2.1 for the 15% conversion level. Therefore the first treatment with the acid has a pronounced effect upon the sample shape-selectivity. This is a rather surprising finding, as all the characterization methods used here did not monitor any anomalous behaviour of the first dealuminated sample. It is also clear that *m*-xylene transformation alone is a very sensitive probe and can discern changes between the samples revealing otherwise similar characteristics.

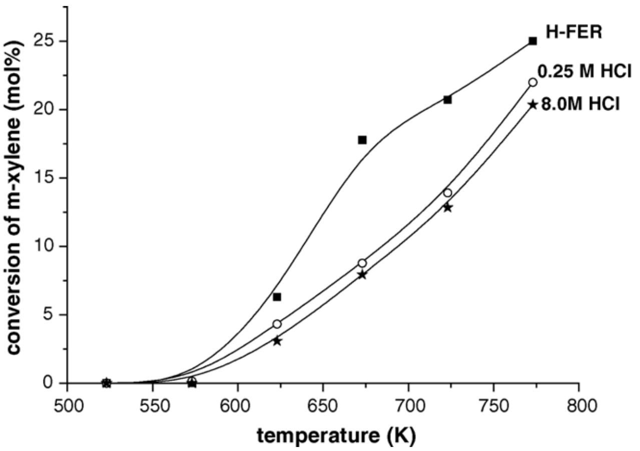

Fig. 6. Conversion of *m*-xylene (mol%) as a function of temperature for the isomerization of the parent H–FER and the two dealuminated catalysts.

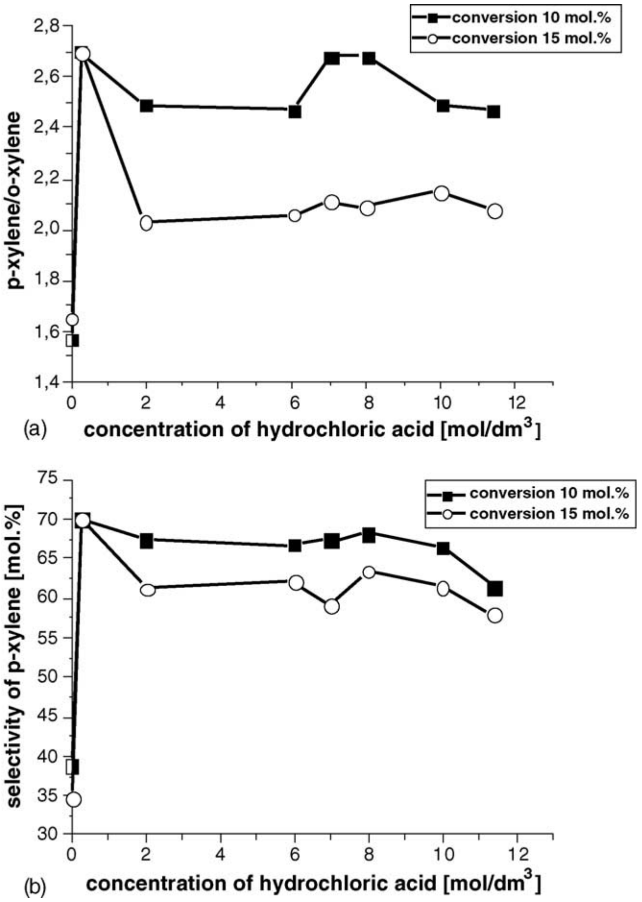

Fig. 7. *p*-Xylene/*o*-xylene ratio (a) and selectivity of *p*-xylene formation (b) on the zeolite H–FER and dealuminated catalysts as a function of HCl concentration (mol/dm^3) for isomerization of *m*-xylene.

The amount of *p*-xylene formed in the reaction is much higher than thermodynamic equilibrium (24%), and is 60–70% depending on the conversion level (Fig. 7b). It seems that the first small portions of aluminium released from the framework tetrahedral positions and giving rise to aluminium gradient in the crystals (Al-rich surface versus Si-rich core) have a predominant influence upon the *m*-xylene transformation route. Interestingly, the tetrahedral aluminium in the ^{27}Al MAS NMR spectrum is completely missing in the sample treated with 8 M HCl, this material exhibits, however, the catalytic activity similar to the other catalysts studied here.

Finally, the dealumination of ferrierite does not exert significant effect on the rate of *m*-xylene isomerization (for all the catalysts a slightly lower activity was observed in comparison the parent sample), but leads to a decrease in the rate of *m*-xylene disproportionation and an increase in the isomerization selectivity, thus giving *p*-xylene rich product. The course of xylenes transformation depends on the zeolite pore system and its geometry. Thus on materials like faujasite, zeolites L and Beta, i.e. aluminosilicates characterised by large-pore system, the isomerization of xylenes is accompanied by parallel transalkylation (disproportionation) of dimethylbenzenes to toluene and trimethylbenzenes. This parallel reaction decreases the overall yield of xylenes, and principally is governed by the intrinsic properties of zeolite and its Si/Al ratio. The formation of *o*-xylene might be also blocked in same zeolites [27], and this process might be invoked here to explain the reaction course. On the other hand, when one restricts steadily the pore diameter and the space needed for the formation of bulky transition-state complexes, the monomolecular isomerization of xylenes starts to dominate. Thus the ratio between the isomerization and disproportionation routes shifts in favour of the previous reaction. Such a situation is found in ZSM-5, and in ferrierite type materials obtained in this work.

4. Conclusions

A treatment of ferrierite type zeolite with hydrochloric acid leads to a continuous depletion of aluminium from tetrahedral framework positions. However, most of the extracted Al remains in the zeolite crystals. This is inevitably accompanied by a rather small crystallinity loss (below 10% for most of the samples), while maintaining very good sorption properties of the modified solids. Small and anisotropic unit cell contraction was also evidenced in a series of the adsorbents studied.

The severity of the treatment (0.25–11.4 M HCl) affects the level of dealumination. The process is monotonous, when applying weak to medium acid solutions. However, there are some phenomena occurring at higher acid concentrations (>6 M). First, dealumination is not so deep after the 11.4 M HCl treatment. Second, the ^{27}Al NMR silent sample was obtained when ferrierite was treated with 8 M HCl solution. It is therefore clear that aluminium in this sample must be highly distorted and thus not seen in a standard NMR experiment.

The selectivity of *m*-xylene transformation depends on the acid treatment. This test reaction was found to be very sensitive and able to monitor subtle changes occurring in a sample treated with a weak mineral acid (0.25 M), and hardly seen by other experimental techniques used. Disproportionation of xylene, giving toluene and trimethylbenzenes, is suppressed in all the dealuminated samples. The selectivity towards *p*-xylene is high and can achieve 60–70% depending on the conversion level.

Acknowledgements

The authors gratefully acknowledge the financial support from the State Committee for Scientific Research, Warsaw, under the project no. 4 T09A 16725 (2003–2005). We also thank F. Bertinchamps (Université Catholique de Louvain, Louvain-la-Neuve, Belgium) for XPS measurements.

References

[1] J. Scherzer, J. Catal. 54 (1978) 285;
J. Scherzer, ACS Symp. Ser. 248 (1984) 157.
[2] B. Sulikowski, Heterogen. Chem. Rev. 3 (1996) 203.
[3] R.M. Barrer, M.B. Makki, Can. J. Chem. 42 (1964) 1481.
[4] B. Sulikowski, J. Rakoczy, H. Hamdan, J. Klinowski, J. Chem. Soc., Chem. Commun. (1987) 1542.
[5] E.F.T. Lee, L.V.C. Rees, J. Chem. Soc., Faraday Trans. 183 (1987) 1531.
[6] J.T. Kim, M.C. Kim, Y. Okamoto, T. Imanaka, J. Catal. 115 (1989) 319.
[7] B. Sulikowski, J. Phys. Chem. 97 (1993) 1420.
[8] J.A. Rabo, R.J. Pellet, A.P. Risch, C.S. Blackwell, in: Proceedings of the Eighth Annual Fluid Catalytic Cracking Symposium Presented at the Katalistiks, Budapest, Hungary, June 1–4, 1987.
[9] J. Čejka, B. Wichterlová, Catal. Rev. 44 (2002) 375.
[10] J.A. Martens, J. Perez-Pariente, E. Sastre, A. Corma, P.A. Jacobs, Appl. Catal. 45 (1988) 85.
[11] J. Dewing, J. Mol. Catal. 27 (1984) 25.
[12] V. Mavrodinova, V. Penchev, U. Lohser, H. Stach, Zeolites 9 (1989) 197.
[13] B. Sulikowski, J. Datka, B. Gil, J. Ptaszynski, J. Klinowski, J. Phys. Chem. B 101 (1997) 6929;
M. Derewiński, S. Dźwigaj, J. Haber, R. Mostowicz, B. Sulikowski, Z. Phys. Chem. (München) 171 (1991) 53.
[14] B.S. Kwak, J. Sung, Catal. Lett. 53 (1998) 125.
[15] S.-H. Lee, D.-K. Lee, C.-H. Shin, W.C. Paik, W.M. Lee, S.B. Hong, J. Catal. 196 (2000) 158.
[16] B. Sulikowski, J. Janas, J. Haber, A. Kubacka, Z. Olejniczak, E. Wloch, Chem. Commun. (1998) 2755.
[17] V. Cortés Corberán, R.X. Valenzuela, B. Sulikowski, M. Derewinski, Z. Olejniczak, J. Krysciak, Catal. Today 32 (1996) 193.
[18] B. Sulikowski, J. Klinowski, J. Phys. Chem. 96 (1992) 5030.
[19] K.-H. Lee, B.-H. Ha, Micropor. Mesopor. Mater. 23 (1998) 211.
[20] J. Kornatowski, W.H. Baur, G. Pieper, M. Rozwadowski, W. Schmitz, A. Cichowlas, J. Chem. Soc., Faraday Trans. 88 (1992) 1339.

[21] P. Cañizares, A. Carrero, Appl. Catal. A: Gen. 248 (2003) 227.
[22] G. Bagnasco, J. Catal. 159 (1996) 249.
[23] K. Góra-Marek, M. Derewiński, P. Sarv, J. Datka, Catal. Today, (2005) in press.
[24] D. Barthomeuf, R. Beaumont, J. Catal. 30 (1973) 288.
[25] F. Lónyi, J. Valyon, Micropor. Mesopor. Mater. 47 (2001) 293.
[26] D.P.B. Peixoto, S.M. Cabral de Menezes, M.I. Pais da Silva, Mater. Lett. 4453 (2003) 1.
[27] D. Seddon, J. Catal. 98 (1986) 1.